ELSEVIER

Chemical Engineering Journal 127 (2007) 81–93

Chemical Engineering Journal

www.elsevier.com/locate/cej

Numerical investigation on the application of catalytic combustion to HCCI engines

Wen Zeng *, Maozhao Xie, Ming Jia

Department of Power Engineering, Dalian University of Technology, Dalian 116024, PR China

Received 23 March 2006; received in revised form 25 August 2006; accepted 3 October 2006

Abstract

The combustion processes of homogeneous charge compression ignition (HCCI) engines whose piston surfaces were coated with catalyst (platinum) are numerically investigated. The detailed reaction mechanism of methane oxidation on platinum catalyst is adopted. Mathematical models of three different levels, namely, a single-zone model, a multi-zone model, and a multidimensional one are developed. The effects of catalytic combustion on the ignition timing, the emissions of hydrocarbon (HC), carbon monoxide (CO) and nitrogen oxide (NO_x), and the combustion characteristics of HCCI engines are analyzed through the single- and the multi-zone models. The results show that due to the catalytic coating the ignition timing is advanced, the emissions of HC and CO are decreased, while the emissions of NO_x are elevated, and that the indicated fuel conversion rate and the combustion efficiency are increased. Furthermore, through the multidimensional model, the inhomogeneity of the temperature and species concentration fields as well as the turbulence effect are considered. It is shown that the temperature and HC, CO concentration fields in the cylinder are more homogeneous because of the effects of catalytic combustion. Finally, a brief comparison of the above three models is presented. Advantages, drawbacks and applicabilities of each model are discussed.

Keywords: Catalytic combustion; HCCI; Single-zone model; Multi-zone model; Multidimensional model; Methane

1. Introduction

With the rapid development of world economy, the problems of energy resource crisis and environment pollution become more and more serious. As one of the main energy consumers and the main source of environment pollution, the automobile receives comprehensive attentions of worldwide researchers. Because of its high efficiency, very low nitrogen oxide (NO_x) and particulate matter emissions, the homogeneous charge compression ignition (HCCI) engine has recently become the focus of engine research. However, the HCCI engine still fronts some challenges including higher hydrocarbon (HC) and carbon monoxide (CO) emissions, control of ignition timing and limited operating range [1–7]. Furthermore, because of the lower exhaust temperature, dealing with the emissions by after-treatment (that is a conventional approach to decrease emissions of internal combustion engines) becomes difficult. So we must find new means to resolve these problems before the HCCI engine can be put into practical applications.

Compared with the traditional combustion mode, catalytic combustion is a different process in which exist complicated interactions between homogeneous and heterogeneous reactions and, there is no flame propagation, and its ignition temperature is lower. For this reason, catalyst coatings on the internal cylinder head, pre-combustion chamber, piston surface and piston crown, can be used to modify the engine combustion process and the combustion characteristics, decrease HC, CO, NO_x emissions and extend the operating range of the internal combustion engine. Gaffney et al. [8] reported that Pt coatings decreased soot emission from a diesel engine by 40%, although the coatings were lost within 8 h of engine operation presumably because of poor adhesion caused by carbon and iron oxide deposits on the piston surface. A “catalytic engine” was described by Thring [9] which consisted of a methanol-burning, modified indirect injection diesel engine where the pre-combustion chamber was fitted with both a glow-plug and Pt mesh catalyst. The results showed that this engine had light-load fuel economy as good as a diesel, and the HC emissions were lower than either petrol or diesel engine. Hu and Ladommatos [10] and Hu [11]

* Corresponding author. Tel.: +86 41184704541; fax: +86 41184708460.
E-mail address: zengwen927@sohu.com (W. Zeng).

1385-8947/$ – see front matter © 2006 Elsevier B.V. All rights reserved.
doi:10.1016/j.cej.2006.10.018

Nomenclature

A	pre-exponential factor
A_s	area of piston surface
A_w	surface area of cylinder wall
B	diameter of bore
$\bar{c}_p$	constant pressure specific heat averaged over all species
c_v	constant volume specific heat
C_j	concentration of species j
D_m	Fick's Law diffusion coefficient
E_a	activation energy
h_j	specific enthalpy of species j
$\mathbf{I}$	unit dyadic
m	mass
p	fluid pressure
p_{cyl}	pressure in the cylinder
$\dot{q}_{loss}$	heat loss of the combustion chamber averaged over the mass in the cylinder
R	gas constant
$\bar{R}$	gas constant averaged over all species
$\dot{s}$	surface reaction rate
S	sticking coefficient
$\bar{S}_p$	average speed of piston
t	time
T	temperature
T_w	temperature of cylinder wall
$\mathbf{u}$	fluid velocity
u_j	internal energy of species j
v	specific volume
v_{st}	Stefan velocity
V_{cyl}	volume of cylinder
$\dot{w}$	gas reaction rate
$\bar{W}$	molecular weight averaged over all species
W_j	molecular weight of species j
Y_j	mass fraction of species j

Greek letters

δ	Diract delta function
λ	second coefficients of viscosity
μ	first coefficients of viscosity
ρ	total mass density
ρ_j	mass density of species j

Subscripts

i	index of zones
j	index of species
$t-1$	previous time step
T	transpose of matrix
2	zone 2

reported that unburned HC emissions were reduced by 20% by the deposition of a catalytic Pt-Rh coatings on the top and side surfaces of the piston in an SI laboratory engine. However, there is another view that catalytic coatings have a negative effect on unburned HC emissions through so-called "catalytic flame quenching" [12]. To clarify this issue, deeper investigations are necessary.

All the above researches concerned only experiments for the application of catalytic combustion to conventional internal combustion engines. Due to the lack of detailed surface reaction mechanism and the limitation of computer capability, numerical simulation of the effects of catalytic combustion on the combustion characteristics of conventional internal combustion engines has not been reported in the open literature. This might attributed to that catalytic combustion is a complicated physical and chemical process which includes surface reaction kinetics, gas reaction kinetics as well as complicated transport phenomena of mass, momentum and energy. In fact, the flow and combustion processes in the conventional internal combustion engine themselves are also highly intricate. Simulation of this combustion process needs sophisticated physical and chemical submodels and vast computer resources.

Recently, with the computer capability advancing, new methods of mathematical simulation developed, detailed reaction mechanisms built, and specially new modes of combustion (such as HCCI) provided, mathematical simulation of this process has become possible and considerable progress has been achieved in this area, from which research work by the groups at Wisconsin, Lund and Sandia are representative [13–15]. Differing from the conventional CI and SI combustion modes, ignition in the HCCI engine occurs at multiple sites simultaneously across the combustion chamber. Once the ignition occurs, the gas mixture is consumed quickly even without discernable flame propagation, so detailed chemical kinetics is usually used to simulate HCCI combustion. Based on this consideration, in modeling the effects of catalytic coatings on the combustion characteristics of the HCCI engine we can focus our attention on the aspect of chemical kinetics process, while the complicated transport phenomena and turbulence effect are not taken into account or treated in a much simplified manner. In this way, the whole problem becomes more maneuverable.

The objectives of this paper are two-fold. The first is to examine the applicability of catalytic combustion to the HCCI engine by numerical modeling. The second is to carry out a comparative study, in which three levels of combustion models, i.e. the single-zone, multi-zone and multidimensional models are used separately to simulate the HCCI combustion under the action of catalyst. In this way, advantages and drawbacks of the three kinds of combustion models concerning their applicabilities to HCCI engines might be clarified. This paper is organized as follows: in the next section, the detailed chemical reaction mechanisms adopted in this work are presented. In Section 3, the effects of catalytic combustion on the ignition timing of the HCCI engine are analyzed based on single-zone model simulations. Because the single-zone model cannot predict the emissions of HC and CO, in Section 4, a multi-zone model is built. The effects of catalytic combustion on HC, CO and NO_x emissions are discussed through this model. In Section 5, through the multidimensional CFD model, the in-cylinder flow field, and the inhomogeneity of temperature and species concentration fields

are considered, and the effects of catalytic combustion on the ignition timing, the temperature and species concentration fields, and HC, CO and NO_x emissions of the HCCI engine are analyzed. In the last section, a brief comparison among the above three models is presented, and conclusions of the paper are given.

2. Chemical kinetic model

2.1. Surface reaction kinetic model

Up to now, detailed surface reaction mechanisms of the hydrocarbon whose carbon atom's number is greater than three have not been built up, and only the detailed surface reaction mechanisms of methane, ethane, and ethene on Pt or Rh surface have been developed. However, as discussed above, detailed chemical kinetics is needed to simulate HCCI combustion. So in this paper, we choose methane as fuel.

As shown in Table 1, the detailed surface reaction mechanism of CH_4 on platinum catalyst consists of 9 gas species, 11 surface species and 26 surface reactions [16]. This reaction mechanism has been verified by results of extensive simulations and experiments [17]. In all simulations of this paper, the surface site density of catalyst coatings is taken as 2.72×10^{-9} mol/cm^2.

2.2. Gas reaction kinetic model

A detailed gas reaction mechanism of methane oxidation is adopted. It consists of 53 species and 325 reactions. This mechanism refers to C/H/O/N chemistry (nitrogen chemistry is included), thus the NO_x emission can be calculated. Through validations by many researchers, good agreements between the simulations and experiments have been obtained [18].

3. Single-zone model simulations

3.1. Physical model

In this section, the HCCI combustion process in an engine of passenger car is simulated. This engine has been usually used in HCCI combustion research [19]. A schematic of the piston is shown in Fig. 1. The specifications and initial conditions of engine are given in Table 2. The top surface of the piston has catalyst Pt coatings. The procedure of coating the catalyst onto the piston surface was detailed discussed in [10].

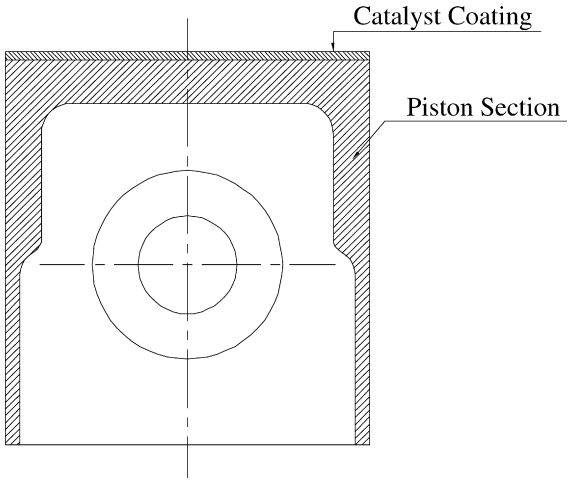

Fig. 1. Schematic of the piston.

Table 1
Surface reaction mechanism of methane on Pt surface

Reactions	S	A (mol cm s)	E_a (kJ/mol)
$H_2 + Pt(s) + Pt(s) \rightarrow H(s) + H(s)$	0.046E−00		0.0
$H + Pt(s) \rightarrow H(s)$	1.000E−00		0.0
$O_2 + PT(s) + Pt(s) \rightarrow O(s) + O(s)$	2.300E−02		0.0
$CH_4 + PT(s) + Pt(s) \rightarrow CH_3(s) + H(s)$	1.000E−02		0.0
$O + Pt(s) \rightarrow O(s)$	1.000E−00		0.0
$H_2O + Pt(s) \rightarrow H_2O(s)$	0.750E+00		0.0
$CO + Pt(s) \rightarrow CO(s)$	8.400E−01		0.0
$OH + Pt(s) \rightarrow OH(s)$	1.000E−00		0.0
$O(s) + H(s) \Leftrightarrow OH(s) + Pt(s)$		3.700E+21	11.5
$H(s) + OH(s) \Leftrightarrow H_2O(s) + Pt(s)$		3.700E+21	17.4
$OH(s) + OH(s) \Leftrightarrow H_2O(s) + O(s)$		3.700E+21	48.2
$CO(s) + O(s) \rightarrow CO_2(s) + Pt(s)$		3.700E+21	105.0
$C(s) + O(s) \rightarrow CO(s) + Pt(s)$		3.700E+21	62.8
$CO(s) + Pt(s) \rightarrow C(s) + O(s)$		1.000E+18	184.0
$CH_3(s) + Pt(s) \rightarrow CH_2(s) + H(s)$		3.700E+21	20.0
$CH_2(s) + Pt(s) \rightarrow CH(s) + H(s)$		3.700E+21	20.0
$CH(s) + Pt(s) \rightarrow C(s) + H(s)$		3.700E+21	20.0
$H(s) + H(s) \rightarrow Pt(s) + Pt(s) + H_2$		3.700E+21	67.4
$O(s) + O(s) \rightarrow Pt(s) + Pt(s) + O_2$		3.700E+21	213.0
$H_2O(s) \rightarrow H_2O + Pt(s)$		1.000E+13	40.3
$OH(s) \rightarrow OH + Pt(s)$		1.000E+13	192.8
$CO(s) \rightarrow CO + Pt(s)$		1.000E+13	125.5
$CO_2(s) \rightarrow CO_2 + Pt(s)$		1.000E+13	20.5

Table 2
Specifications and initial conditions of the engine

Bore (mm)	Stroke (mm)	Connecting rod length (mm)	Engine speed (rpm)	Compression ratio	Initial temperature (K)	Initial pressure (bar)	λ	Fuel
89	105.8	169.1	2500	15.0	500	1	3.3	CH_4

3.2. Computational model

The single-zone model is used to analyze the effects of catalytic combustion on the ignition timing of the HCCI engine. In this model, thermodynamic properties are assumed uniform throughout the chamber volume. The computation starts from IVC.

The basic equations of this model are as follows:

Conservation of energy

$$\frac{dT}{dt} = \frac{\dot{q}_{loss} - (RT/v\bar{W})\ dv/dt - v\sum_{j=1}^{K} u_j W_j \dot{w}_j - \sum_{j=1}^{K} u_j \dot{s}_j W_j (A_s/m)}{c_v} \quad (1)$$

Conservation of species

$$\frac{dY_j}{dt} = vW_j\dot{w}_j + \frac{A_s}{m}\dot{s}_j W_j \quad (2)$$

where K is the total number of gas phase species, the gas reaction rate is computed by CHEMKTN package [20], while the surface reaction rate is computed by DETCHEM package [21]. The specific cylinder volume is specified as a function of crank angle (°) [22].

The heat loss from the combustion chamber can be computed by the Woschni [23] heat transfer model given as:

$$\dot{q}_{loss} = \frac{hA_w(T - T_w)}{m} \quad (3)$$

The heat transfer coefficient h can be calculated by

$$h = 129.8B^{-0.2}p_{cyl}^{0.8}T^{-0.55}w^{0.8} \quad (4)$$

The average gas velocity w can be calculated by

$$w = C_1\bar{S}_p + C_2\frac{V_{cyl}T_r}{p_r V_r}(p_{cyl} - p_{mot}) \quad (5)$$

where T_r, p_r and V_r are referenced temperature, pressure and volume, respectively. C_1 is 2.28. C_2 is 0 for compression and 3.34×10^{-3} for combustion and expansion.

3.3. Computational results

3.3.1. Effects of catalytic combustion on the ignition timing of the HCCI engine

As shown in Fig. 2, the ignition timing is advanced with catalyst coatings on the piston surface. The ignition timing is 372 °CA without catalyst coatings, while it is 364 °CA with Pt catalyst coatings on the piston surface. Furthermore, with the ignition timing advancing, the peak temperature in the cylinder is elevated slightly. The peak temperature in the cylinder is 1970 K without catalyst coatings, and is 2000 K with Pt catalyst coatings on the piston surface. The peak temperature is only elevated by 30 K.

For HCCI engines, one of the most important problems is the control of the ignition timing. Some control mechanisms such as alterations of the initial pressure and temperature, variable compression ratio and exhaust gas re-circulation (EGR) have potentials for controlling combustion timing [6]. However, by these means, with the ignition timing advanced or delayed slightly, the peak temperature will be elevated or dropped greatly. If the peak temperature in the cylinder is elevated greatly, engine knock may be produced to mangle the engine and the emissions of NO_x would be enhanced. On the other hand, if the peak temperature in the cylinder falls greatly, incomplete combustion will happen, which would enhance the HC emissions. In the case of catalytic combustion the situation is different, as shown in Fig. 2, with the ignition timing advancing, the peak temperature is elevated only slightly with the catalyst coatings. Hence, in the view of controlling the ignition timing, one might draw some inspiration from the catalytic coating effect.

4. Multi-zone model simulations

The single-zone model is very useful for investigating the ignition timing, however, it provides little information about the period following ignition, as it assumes that the entire cylinder charge is homogeneous and therefore greatly over predicts the combustion rate and the emission of NO_x. In an effort to describe the physical processes occurring in the cylinder more detailedly and predict the emissions more accurately, a multi-zone model

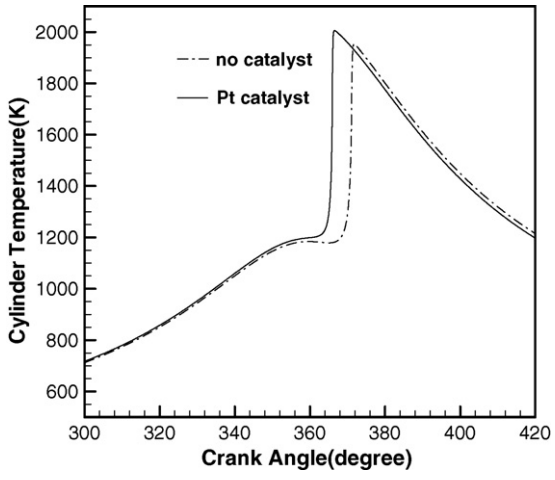

Fig. 2. Effects of catalytic combustion on the ignition timing of the HCCI engine.

Table 3
Specifications and initial conditions of the engine

Bore (mm)	89
Connecting rod length (mm)	169.1
Stroke (mm)	105.8
Compression ratio	15:1
Engine speed (rpm)	2500
Crevice volume (cm^2)	1.65
Quench layer thickness (mm)	1
Wall temperature (K)	390
Air excess ratio	3.3
Initial pressure (bar)	1

is developed to simulate the effects of catalytic combustion on the emissions of CO, HC and NO_x. Although it is not intended to be a "predictive" model of HCCI ignition and emissions, the computation times are relatively short in comparison with the multidimensional model (which will be discussed in the next section) while still providing valuable information about HCCI ignition and combustion processes.

4.1. Physical model

The main specifications of the HCCI engine simulated in this paper are listed in Table 3.The engine used in this section is the same one as used in the single-zone model. Initial conditions of the multi-zone model are listed in Table 4. The principle of the initial mass and temperature distributions throughout the zones was detailedly discussed in [24].

A schematic of the engine cylinder and zone definitions is shown in Fig. 3. Note that only the piston top surface has Pt catalyst coatings.

4.2. Computational model

In this paper, six zones are used to provide some details, but without extraordinarily long running times. The zones are defined such that they are representative of the crevice, boundary layer, outer core, and inner core regions, respectively. The three inner core regions are considered to be adiabatic. Heat loss to the walls from the boundary layer zone is modeled using the Woschni correlation and the temperature of crevice zone is considered to remain constant and equal to the wall temperature throughout the cycle. The outer core, boundary layer, and crevice region are allowed to exchange mass in order to maintain a uniform pressure throughout the combustion chamber. The inner three core zones are assumed to be of constant mass so that when

Table 4
The initial mass and temperature distributions of zones

Zones	Mass fraction	Temperature (K)
1	0.3	390
2	6.6	435
3	52.2	455
4	14.5	470
5	16.4	495
6	10.0	520

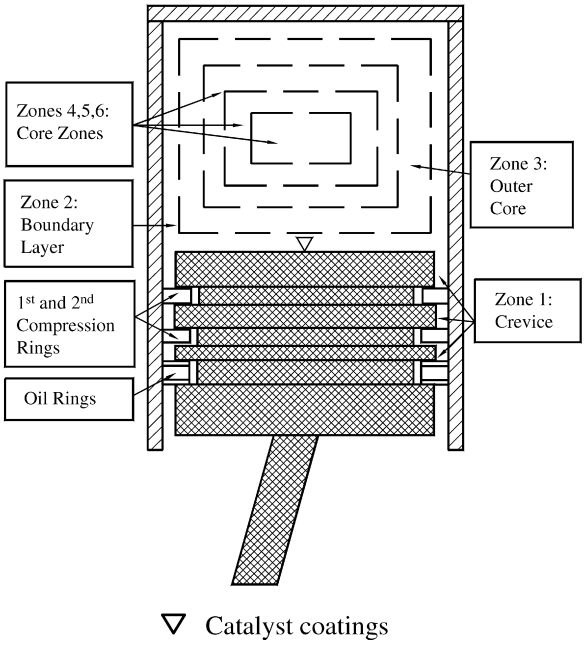

Fig. 3. Multi-zone model schematic showing the layout of the zones.

combustion started these regions simply expand without mixing with other zones. Mass that flows from the outer core must pass through the boundary layer before entering the crevice region and that leaving the crevice must also flow through the boundary layer before entering the outer core. Mass transferred between these zones is considered to instantly mix with the mass already present in the zone it is entering.

The basic equations of this model are as follows:

Conservation of energy

$$\bar{c}_{p,i}\frac{\mathrm{d}T_i}{\mathrm{d}t} - \bar{R}_i T_i \frac{\sum_{i=1}^{N} m_i \bar{R}_i \ \mathrm{d}T_i/\mathrm{d}t}{\sum_{i=1}^{N} m_i \bar{R}_i T_i} = \dot{q}_i - R_i T_i \frac{1}{V_{\mathrm{cyl}}}\frac{\mathrm{d}V_{\mathrm{cyl}}}{\mathrm{d}t} \tag{6}$$

Conservation of species

$$\frac{\mathrm{d}Y_{j,i}}{\mathrm{d}t} = v_i W_{j,i}\dot{w}_{j,i} + \frac{A_{\mathrm{s}}}{m_2}\dot{s}_{j,2}W_{j,2} \tag{7}$$

Ideal gas law

$$p_{\mathrm{cyl}} = \frac{\sum_{i=1}^{N} m_{i,t-1}\bar{R}_i T_i}{V_{\mathrm{cyl}}} \tag{8}$$

where N is the total number of elementary reactions, $\dot{q}_i$ the sum of the chemical heat release and the heat transfer to the wall of the unit mass in zone i, the chemical heat release consists of those from gas reactions and surface reactions.

Because the volumes of the crevice, boundary layer, and outer core zone have been adjusted to fit our definitions without considering mass transfer between them, pressure differences will exist between these zones. Therefore mass must be transferred between these zones, the pressure in each of the zones is calculated using the ideal gas law, and the directions of flow are determined from the pressure differences. Mass flows from

zones of higher pressure to those of lower pressure and in this manner the pressure in each of the three zones equalizes to the overall cylinder pressure. The mass flowing between zones contains energy and does work in moving across the zone boundaries.

At each time step the pressure in each zone keeps unchanged. Pressure differences in the zones only exist during the intermediate step of solving for the conditions at time t. Since very small time step are taken, the solution will closely approximate the actual solution.

4.3. Computational results

4.3.1. Effects of catalytic combustion on temperature and heat release in the cylinder

As shown in Fig. 4, catalytic combustion has little effect on the temperatures of zones 1 and 4–6, but has effects on those of zones 2 and 3. The main reason is that the temperature of zone 1 is considered to equal constantly to the wall temperature, and zones 4–6 are the inner core zones, which do not exchange mass with other zones. In our simulations, because only in zone 2 that has Pt catalyst coatings, the chemical reaction is accelerated by the catalytic effect, consequently, the temperature of this zone is higher than that when the piston surface has no catalyst coatings. Because of the mass exchange between zones 2 and 3, the temperature of zone 3 is also affected by catalytic combustion. Comparing with the case without catalyst coatings, the ignition timing of zone 3 is advanced, and the peak temperature is remarkably elevated.

As shown in Fig. 5, because in zone 2 the gas mixture is never ignited throughout the whole process, the catalytic coating can only induce a marginal increase in the temperature but has no effect on the heat release of zone 2. On the other hand, the heat release of zone 3 is much higher compared with the case without catalyst coatings.

4.3.2. Effects of catalytic combustion on HC emissions

Zones 4–6 are inner core zones, there are no mass exchange among these three zones and other zones, and the temperatures

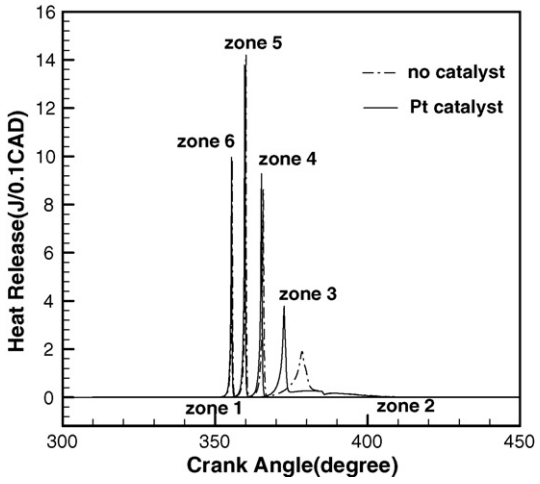

Fig. 5. Effects on heat releases of all zones.

of these three zones are the highest among all the six zones, thus the unburned HC mass fractions in these three zones are slight. The expansion leads to unburned mixture flowing from zone 2 into zone 3, because of the low temperature, the reaction in zone 3 is slow, resulting in a small quantity of HC here. The temperatures of zones 1 and 2 are much lower, thus plenty of HC exists in these two zones. On the other hand, with the catalyst coatings on the piston surface, the reaction rate of zone 2 is accelerated, and the temperatures of this zone is elevated, as shown in Fig. 6, so the HC mass fraction of this zone is slightly reduced. As shown in Fig. 7, because zones 1–3 are the main source of HC production, compared with the case of no catalyst coatings, the HC total mass fraction is reduced by about 5% with Pt catalyst coatings on the piston surface.

4.3.3. Effects of catalytic combustion on NO_x emissions

In zones 4–6, complete combustion takes place, hence, the temperatures of these three zones are very high, consequently, they are the main sources of the NO_x emissions. Fig. 8 shows that with Pt catalyst coatings on the piston surface, the reaction rates are accelerated and the temperatures of zones 4–6 are elevated, the NO_x mass fractions of zones 4–6 are increased because the

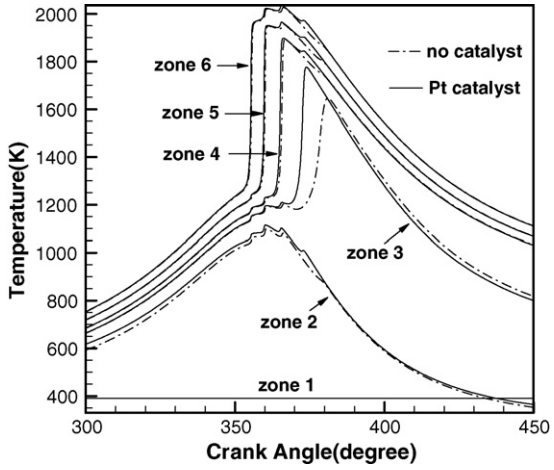

Fig. 4. Effects on temperatures of all zones.

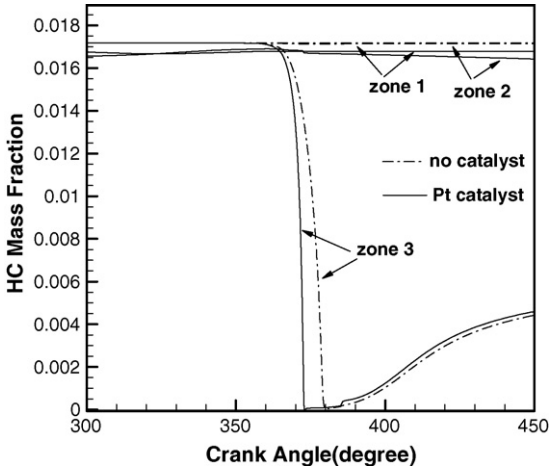

Fig. 6. Effects on HC mass fractions (zones 1–3).

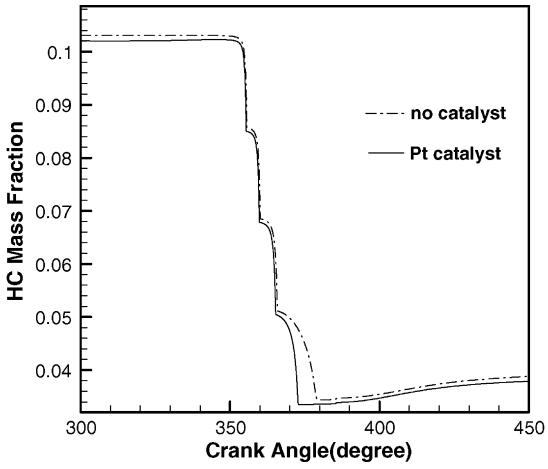

Fig. 7. Effects on the total HC mass fraction.

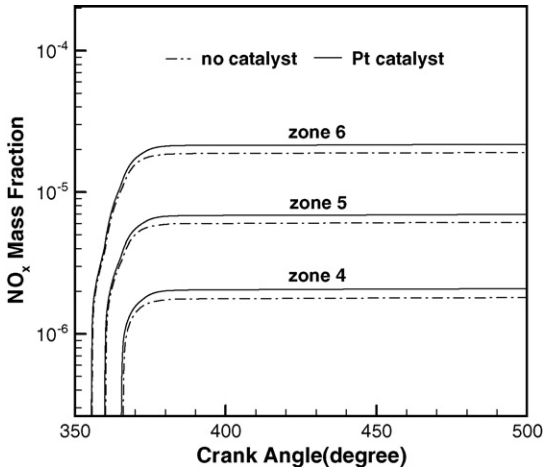

Fig. 8. Effects on NO_x mass fractions (zones 4–6).

NO_x emission is an exponential function of temperature. Zones 1–3 are not included in this graph because temperatures in these zones are not high enough to have significant NO_x formation. As shown in Fig. 9, compared with no catalyst coatings, the total NO_x mass fraction is elevated by 5% with Pt catalyst coatings on the piston surface.

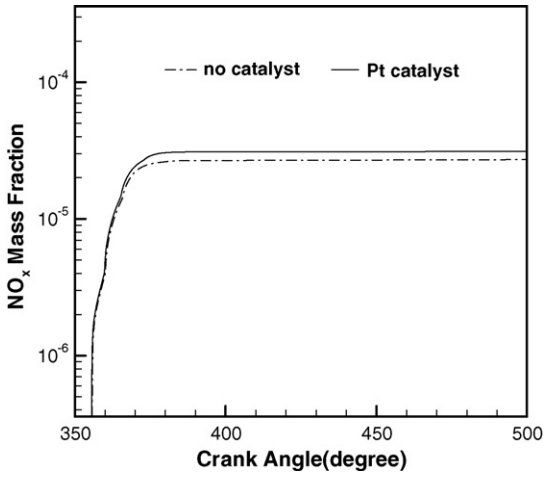

Fig. 9. Effects on the total NO_x mass fraction.

4.3.4. Effects of catalytic combustion on CO emissions

Zones from 4 to 6 are the main combustion zones. Almost all CO formed in these three zones during the early stages of combustion is converted to CO_2. The CO formed in the initial stage of combustion in zone 3 is also converted to CO_2, but the unburned mixture that enters zone 3 from zone 2 during the expansion stroke results in another source of CO emissions. Part of the unburned mixture reacts to form CO, some of which is further oxidized to form CO_2. However, because of decreasing temperature in zone 3 during expansion, the rate of CO oxidation rate is very small resulting in a large amount of CO. The temperatures of zones 1 and 2 are quite low, so the reaction proceeds slowly resulting in a small CO mass fraction.

In the combustion process, from the gas mixture to the CO production, as well as from CO to CO_2, CO is only an intermediate species. When the temperature of a zone is lower, with increasing temperature the gas mixture oxidation is accelerated, and the CO mass fraction is increased. However, if the temperature of a zone becomes high enough, the conversion from CO to CO_2 is boosted up, and the CO mass fraction is decreased with increasing temperature. The temperatures of zones 1 and 2 are very low, which are elevated by catalytic combustion, and the reaction in these two zones are accelerated, so the CO mass fractions are increased, as shown in Fig. 10. The temperature of zone 3 is higher, which is also elevated by catalytic combustion, however the oxidation of CO to CO_2 is accelerated too, as indicated in Fig. 11, the CO mass fraction in this zone is decreased. Because zone 3 is the main source of CO emissions, comparing with no catalyst coatings, the total CO mass fraction in the cylinder is reduced with Pt catalyst coatings on the piston surface.

4.3.5. Effects of catalytic combustion on combustion characteristics

Fig. 12 presents a comparison of several combustion performance parameters between the cases with and without catalyst coatings. Compared with the no catalyst case, the average effective pressure is increased by 5%, the indicated fuel conversion rate is increased by 4%, the combustion efficiency is increased

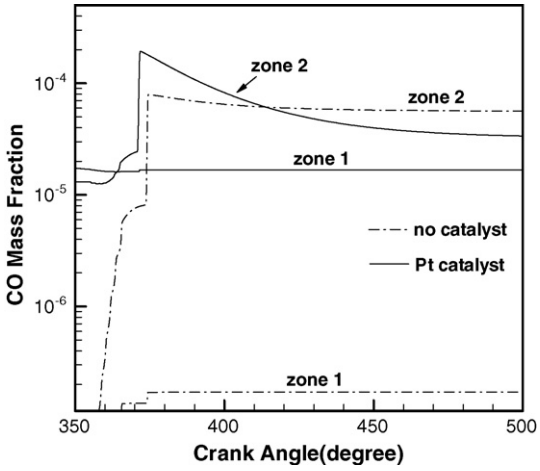

Fig. 10. Effects on CO mass fractions (zones 1 and 2).

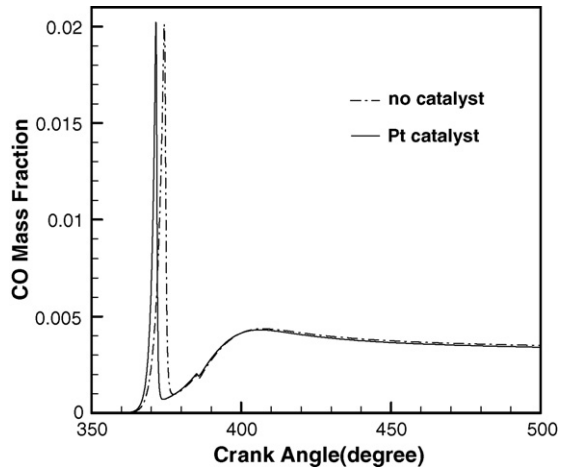

Fig. 11. Effects on the CO mass fraction (zone 3).

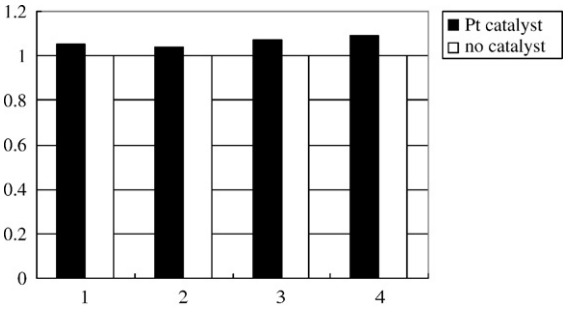

Fig. 12. Effects of catalytic combustion on combustion capabilities (comparisons between without and with Pt coatings 1: average effective pressure, 2: indicated fuel conversion rate, 3: combustion efficiency, 4: burn duration time).

by 7%, and the burn duration time is increased by 9% (since the ignition timing is advanced while the later combustion time is not effected), respectively, with Pt catalyst coatings on the piston surface. This implies that, with Pt catalyst coatings, not only the emissions of HC and CO are decreased, the engine combustion characteristics (the indicated fuel conversion rate and the combustion efficiency) are also improved.

5. Multidimensional model simulations

5.1. Physical model

The engine used for the multidimensional modeling is derived from a Cummins B-series production diesel engine, which is equipped with a custom HCCI piston as shown in Fig. 13. The

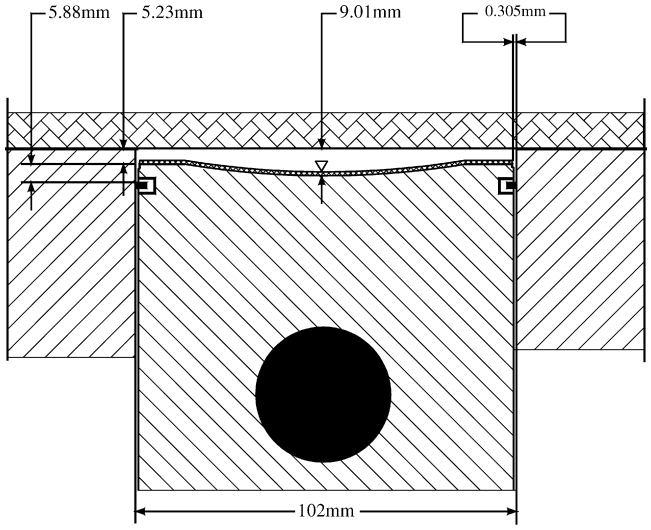

Fig. 13. Schematic of the piston.

specifications of the Cummins B-series production diesel engine are listed in Table 5 [25].

5.2. Computational model

Because ignition in the HCCI engine occurs at multiple sites simultaneously across the combustion chamber, once the ignition occurs, the gas mixture is consumed quickly even without discernable flame propagation. It is generally accepted that the HCCI combustion is dominated by chemical kinetics and turbulence has little direct effect on HCCI combustion. This would be true if a strictly homogeneous mixture exists at the time of combustion. For this reason, detailed chemical kinetics is usually used to simulate HCCI combustion. In the single-zone model and the multi-zone model, the detailed flow field is not considered and the chemical reactions are assumed to be unaffected by flow turbulence. However, some researchers have reported that the flow field in the cylinder had some effects on the rates of chemical reactions and the combustion process of HCCI engines [26–28]. This is because there are always small differences in the temperature and concentration inside the cylinder. To take into account this inhomogeneity effect, a multidimensional model is necessary.

In this section, the CHEMKTN chemistry solver and the DETCHEM surface reaction solver are integrated into the KIVA-3V code for solving the chemistry in coupling with multidimensional engine CFD simulations. The KIVA code is used to

Table 5
Specifications of the Cummins B-series engine

Bore (mm)	Compression ratio	Connecting rod length (mm)	Engine speed (rpm)	EVO	IVC
102	17.0	192	1200	60 BBDC	25 ABDC
Stroke (mm)	Intake temperature (K)	Air excess ratio	Intake pressure (bar)	Wall temperature (K)	Fuel
120	470	3.0	1	400	CH_4

compute the flow field, including the distributions of mass and temperature in the cylinder, CHEMKTN is used to simulate the gas reactions, and DETCHEM is used to simulate the surface reactions.

The KIVA code solves numerically a set of differential equations governing the in-cylinder processes as follows [29]:

The continuity equation for species j:

$$\frac{\partial \rho_j}{\partial t} + \nabla \cdot (\rho_j \mathbf{u}) = \nabla \cdot \left[\rho D_{\mathrm{m}} \nabla \left(\frac{\rho_j}{\rho} \right) \right] + \dot{\rho}_j^{\mathrm{c}} + \dot{\rho}^{\mathrm{s}} \delta_{jl} \tag{9}$$

where $\dot{\rho}_j^{\mathrm{c}}$ and $\dot{\rho}^{\mathrm{s}}$ are source terms due to chemistry and the fuel spray, $\dot{\rho}_j^{\mathrm{c}}$ can be calculated by

$$\frac{\dot{\rho}_j^{\mathrm{c}}}{\rho} = \frac{\mathrm{d}Y_j}{\mathrm{d}t} = v W_j \dot{w}_j + \frac{A_{\mathrm{s}}}{m} \dot{s}_j W_j \tag{10}$$

The boundary condition required at the catalyst-wall is that the gas-phase species mass flux produced by heterogeneous chemical-reaction must be balanced by the diffusive flux of that species in the gas:

$$s_j M_j = \mathbf{j}_j + \rho Y_j v_{\mathrm{st}} \tag{11}$$

where the diffusion flux of species j is calculated by:

$$\mathbf{j}_j = -D_{m,j} \frac{\partial c_j}{\partial r} \tag{12}$$

The momentum equation for the fluid mixture:

$$\frac{\partial (\rho \mathbf{u})}{\partial t} + \nabla \cdot (\rho \mathbf{u}\mathbf{u}) = \frac{1}{\alpha^2} \nabla p - A_0 \nabla \left(\frac{2}{3 \rho k} \right) + \nabla \cdot \boldsymbol{\sigma} + \mathbf{F}^{\mathrm{s}} + \rho \mathbf{g} \tag{13}$$

where the dimensionless quantity α is used in conjunction with the Pressure Gradient Scaling (PGS) Method. A_0 is zero in laminar calculations and unity when one of the turbulence models is used. $\mathbf{F}^{\mathrm{s}}$ is the rate of momentum gain per unit volume due to the spray. The specific body force $\mathbf{g}$ is assumed constant. The viscous stress tensor $\boldsymbol{\sigma}$ can be calculated by

$$\boldsymbol{\sigma} = \mu [\nabla \mathbf{u} + (\nabla \mathbf{u})^T] + \lambda \nabla \cdot \mathbf{u} \mathbf{I} \tag{14}$$

The internal energy equation:

$$\frac{\partial (\rho I)}{\partial t} + \nabla \cdot (\rho \mathbf{u} I) = -p \nabla \cdot \mathbf{u} + (1 - A_0) \boldsymbol{\sigma} : \nabla \mathbf{u} - \nabla \cdot \mathbf{J} + A_0 \rho \varepsilon + \dot{Q}^{\mathrm{c}} + \dot{Q}^{\mathrm{s}} \tag{15}$$

where I is the specific internal energy, exclusive of chemical energy. $\dot{Q}^{\mathrm{c}}$ and $\dot{Q}^{\mathrm{s}}$ are the source terms due to chemical heat release and spray interactions. The heat flux vector $\mathbf{J}$ is calculated as

$$\mathbf{J} = -K \nabla T - \rho D_{\mathrm{m}} \sum_j h_j \nabla \left(\frac{\rho_j}{\rho} \right) \tag{16}$$

When the k–ε turbulence model is in use, two additional transport equations are solved for the turbulent kinetic energy k and its dissipation rate ε

$$\frac{\partial (\rho k)}{\partial t} + \nabla \cdot (\rho \mathbf{u} k) = -\frac{2}{3} \rho k \nabla \cdot \mathbf{u} + \boldsymbol{\sigma} : \nabla \mathbf{u} - \nabla \cdot \left[\left(\frac{\mu}{Pr_k} \right) \nabla k \right] - \rho \varepsilon + \dot{W}^{\mathrm{s}} \tag{17}$$

$$\frac{\partial (\rho \varepsilon)}{\partial t} + \nabla \cdot (\rho \mathbf{u} \varepsilon) = -\left(\frac{2}{3} c_{\varepsilon_1} - c_{\varepsilon_1} \right) \rho \varepsilon \nabla \cdot \mathbf{u} + \nabla \cdot \left[\left(\frac{\mu}{Pr_\varepsilon} \right) \nabla \varepsilon \right] + \frac{\varepsilon}{k} (c_{\varepsilon_1} \boldsymbol{\sigma} : \nabla \mathbf{u} - c_{\varepsilon_2} \rho \varepsilon + c_{\mathrm{s}} \dot{W}^{\mathrm{s}}) \tag{18}$$

where $\dot{W}^{\mathrm{s}}$ is a source term due to the fuel spray. c_{ε_1}, c_{ε_2}, c_{ε_3}, Pr_k and Pr_ε are constants whose values are determined from experiments and some theoretical considerations.

The computation is implemented as follows. At first, because the KIVA code is short of the thermodynamic information of species, the CHEMKIN and DETCHEM interpreters read the mechanism of gas and surface reactions, and the thermodynamic information of species. At the same time, these two interpreters translate the thermodynamic information of species from NASA format to JANAF format for KIVA code. In the computing course of flow field and combustion, the KIVA code provides CHEMKIN and DETCHEM with the information of species, temperature and pressure in each computational cell as initial condition, the CHEMKIN and the DETCHEM solvers then compute the species and heat release in a new time step δt. Afterwards, we return to KFVA to compute the flow field again.

The computation starts from intake valve closure (IVC) to exhaust valve open (EVO), and the distributions of temperature, pressure and species are assumed to be homogenous at the time of intake valve closure. The computing mesh at IVC is shown in Fig. 14. Because Pt catalysts are coated on the piston surface, in order to simulate the effects of catalysis on HCCI combustion process, we only need to compute surface reactions in the meshes adjoining the piston surface.

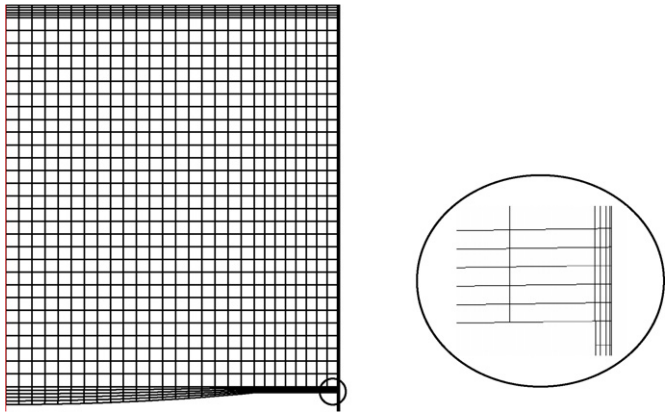

Fig. 14. The computing mesh at 25 ABDC.

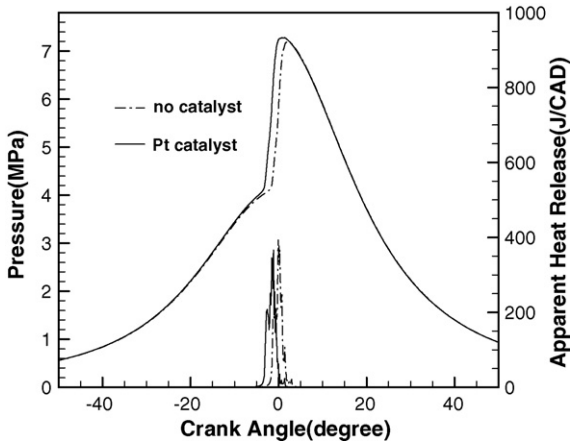

Fig. 15. Effects of catalytic combustion on pressure and heat release.

5.3. Computational results

5.3.1. Effects of catalytic combustion on the ignition timing of the HCCI engine

From Fig. 15 it is clear that the ignition timing is advanced with Pt catalyst coatings on the piston surface. The ignition timing is 1 °CA before top dead center (BTDC) without catalyst, while it is 3 °CA BTDC with Pt catalyst coatings on the piston surface. With the ignition timing advancing, the peak pressure in the cylinder is elevated, which is 7.1 and 7.2 MPa for the cases without and with Pt catalyst coatings on the piston surface, respectively. The peak pressure is elevated by 0.1 MPa due to the catalytic effect.

5.3.2. Effects of catalytic combustion on the temperature field of the HCCI engine

As shown in Fig. 16a1 and a2, at 5 °CA BTDC, the mixed gas in the whole cylinder cannot be ignited for both cases of the piston surface without and with Pt catalyst coatings. However, it should be noted when the piston surface is coated with Pt catalyst, both the peak temperature of the core region and the lowest temperature in crevice region are elevated. At 0 °CA BTDC, as shown in Fig. 16b1, in the case without catalyst, there is a significant temperature gradient in the cylinder, which means that a high temperature region exists in the core region, while in the crevice region and the boundary layer, temperatures are much lower. On the other hand, as shown in Fig. 16b2, when the piston surface coated with Pt catalyst, the temperature field in the cylinder has become essentially homogeneous with considerably elevated temperatures in the boundary layer and the crevice region.

Compared with the conventional SI engine, one of the main advantages of the HCCI engine is that the gas mixture is ignited simultaneously at multiple locations inside the cylinder and the temperature field is overall homogeneous. However, as shown in Fig. 16b1, due to the turbulence effect, there is still a substantial temperature gradient in the cylinder. On the other hand, when the piston surface coated with Pt catalyst, as shown in Fig. 16b2, the homogeneity of temperature field is facilitated by the catalysis, so the feasibility of engine knock is diminished and the emissions of HC and CO could be decreased (which will be detailedly discussed in the next section).

5.3.3. Effects of catalytic combustion on the CO concentration field of the HCCI engine

As shown in Fig. 17a1, at 0 °CA BTDC, when the piston surface has no catalyst, the core temperatures are rather high, and most of the mixed gas in the core region is consumed to form CO_2. Because of low temperature in the crevices, the mixed gas cannot be ignited. Consequently, there only unburned HC is produced. Thus the CO concentrations in these two regions are low. The temperature in the boundary layer is not very high, CO produced by the oxidation of mixed gas cannot be oxidized and converted completely to CO_2, and hence, there is a large CO concentration in the boundary layer. Fig. 17a2 shows that for the piston surface coated with Pt catalyst, the CO concentration in the whole cylinder is higher and more homogeneous because of the higher temperature level and the homogeneity of temperature field. At 120 °CA ATDC, as shown in Fig. 17b1 and b2, although little difference in the CO concentration fields can be observed between the above two cases, there is still some difference in the peak and the lowest CO concentrations. Comparing with no catalyst, the peak and the lowest CO concentrations are lowed in the case with Pt catalyst coatings on the piston surface.

5.3.4. Effects of catalytic combustion on the HC concentration field of the HCCI engine

The calculated HC concentration fields in the cylinder are presented in Fig. 18. As shown in Fig. 18a1, at 0 °CA BTDC, for the case without catalyst, because of high temperature in the core region, there the HC concentration is slight. However, the

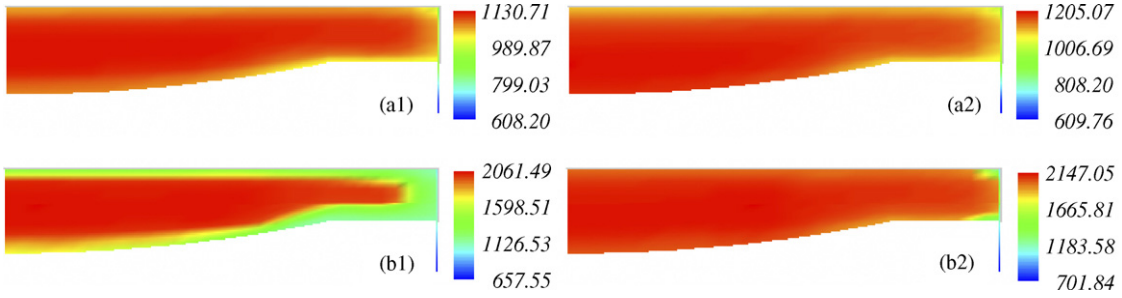

Fig. 16. Effects of catalytic combustion on the temperature (K) field in the cylinder. (a1 and a2) Without and with Pt catalyst on the piston surface at 5 °CA BTDC. (b1 and b2) Without and with Pt catalyst on the piston surface at 0 °CA BTDC.

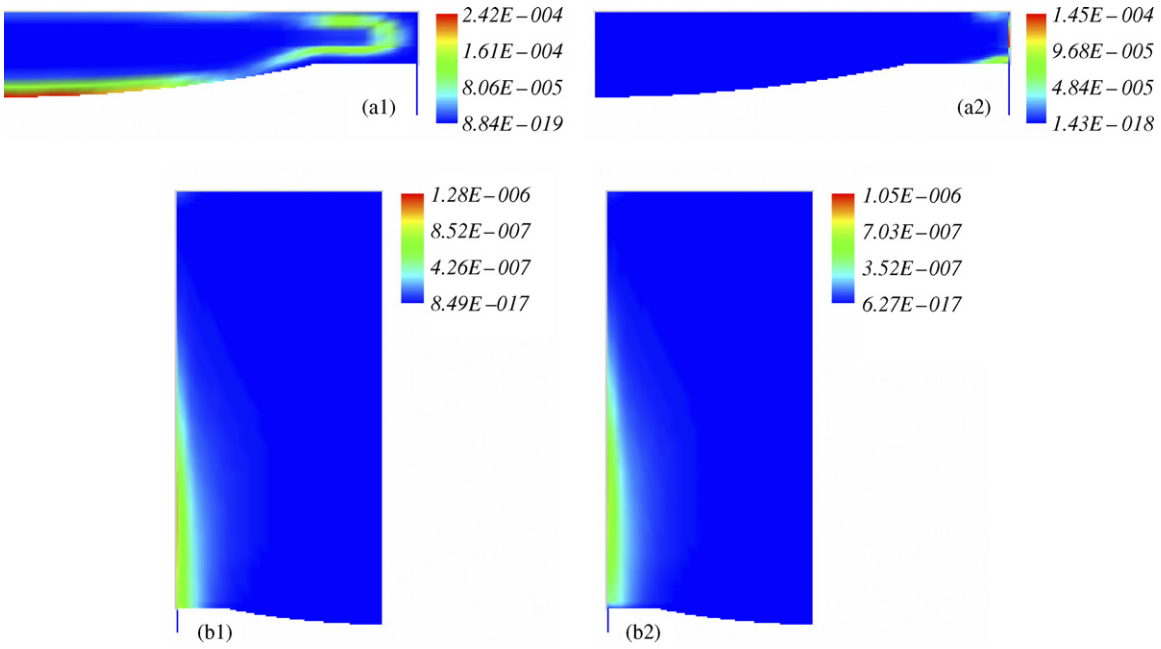

Fig. 17. Effects of catalytic combustion on the CO concentration field in the cylinder. (a1 and a2) Without and with Pt catalyst on the piston surface at 0 °CA BTDC. (b1 and b2) Without and with Pt catalyst on the piston surface at 120 °CA ATDC.

temperatures are low in the regions adjacent to the head and wall of the cylinder as well as to the crevices, the mixtures cannot be oxidized entirely, so there exists a large amount of unburned HC. Contrastively, Fig. 18a2 shows that for the piston surface coated with Pt catalyst, the HC concentrations in the whole cylinder is low and distributed homogeneously because of the high temperature and its homogeneity throughout the combustion chamber. At 120 °CA ATDC, as shown in Fig. 18b, although the HC concentration fields in the above two cases seem similar, there is still certain difference in the peak and the lowest HC concentrations. Comparing with no catalyst, both the peak and the lowest HC concentrations are lower in the case with Pt catalyst coatings on the piston surface. Differing from our results, Hultqvist et al. [12] reported that the catalytic coatings give rise to more unburned HC. The observed HC rising is attributed to the so-called catalytic flame quenching, the mechanism of which is explained as follows. The catalyst coatings have two effects on HC emissions. On one hand, the catalyst coatings affect the thermal boundary layer. The pores in the catalyst coatings enlarge the area of heat transfer and change the heat transfer coefficient.

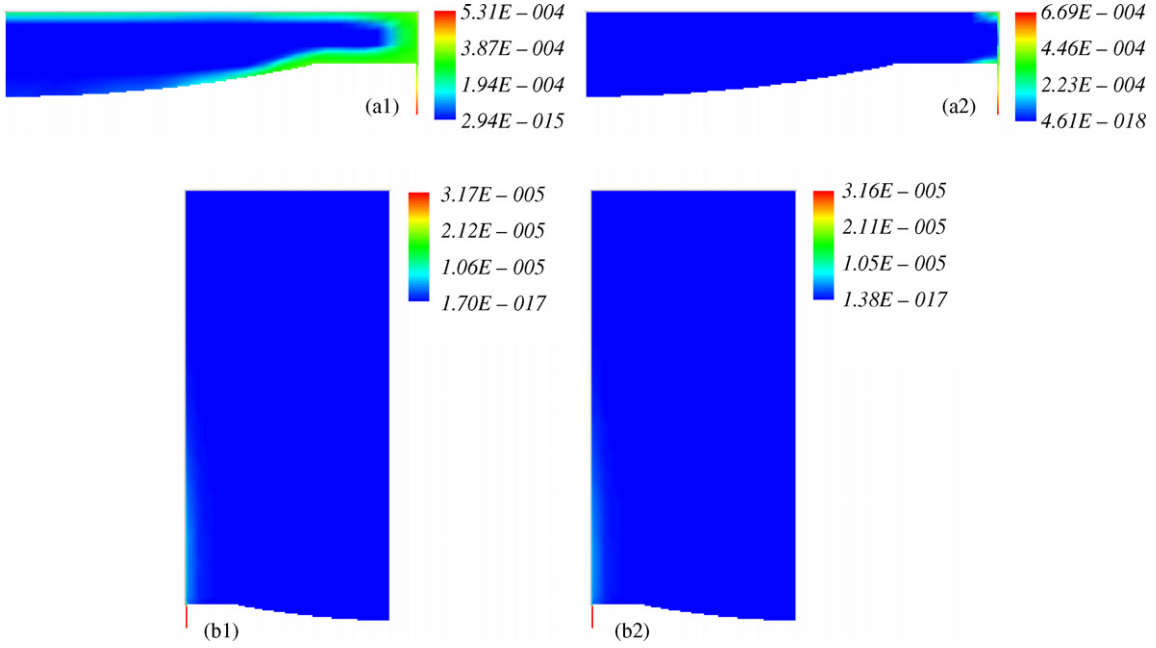

Fig. 18. Effects of catalytic combustion on the HC concentration field in the cylinder. (a1 and a2) Without and with Pt catalyst on the piston surface at 0 °CA BTDC. (b1 and b2) Without and with Pt catalyst on the piston surface at 120 °CA ATDC.

Table 6
Comparisons of the three models

Model	Application range	Compute time
Single-zone	Ignition timing (accurate), emissions of NO_x (higher)	2 min
Multi-zone	Emissions of HC, CO, and NO_x (not very accurate)	4 h
Multi-dimension	Ignition timing and emissions of HC, CO, and NO_x	67 h

Thus, heat transfer in the regions with catalyst coatings becomes stranger and if the heat loss to the walls is greater than the production and convection of heat, the catalytic flame quenching is happened. On the other hand, the catalyst coatings affect the gas reactions confined to it. As discussed in the above section, the catalysis can accelerate the gas reaction rate, so the temperature in the regions adjoining to the catalyst coatings can be elevated. In [12], the upper part of the cylinder liner, the piston top including the top land, the valves and the cylinder head were all coated with Pt catalyst. Hence, from the above mentioned two effects, the first one is dominated. However, in our study, the catalyst is coated only on the piston top surface, but not in the crevice zone, as in the experiment by Hultqvist et al. Thus, the effect of flame quenching should be much weaker than in [12]. Moreover, in our simulation the heat transfer equations and corresponding boundary conditions were not modified to account for the effect of heat transfer enhancement by the porous structure of the catalytic coatings. This would further weaken the wall quenching. For these reasons, the HC emissions predicted by our computation are lower.

5.3.5. Summary of catalytic coating effects on emissions of the HCCI engine

Fig. 19 presents a general comparison of total emission characteristics between the engines with and without catalyst coatings. It can be seen that at the same working conditions, compared with the no catalyst case, the emissions of HC and CO are decreased by 4 and 9%, respectively, with Pt catalyst coatings on the piston surface, while the NO_x emissions increased roughly by 8%. As we know, the NO_x emissions of the HCCI engine are much lower than that of ordinary CI and SI engines, thus with Pt catalyst coatings on the piston surface, a slight increase in the NO_x emissions seems not to deteriorate the advantages of the HCCI engine. Moreover, with catalyst coatings on the piston surface, the emissions of HC and CO are decreased, so the main disadvantage that the HCCI engine has higher HC and CO emissions than conventional engines can be alleviated to some extent.

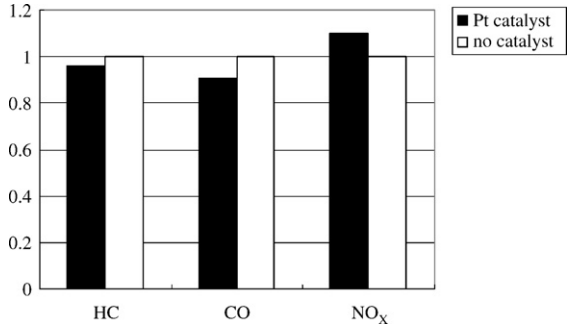

Fig. 19. The emissions of HC, CO and NO_x (comparisons between without and with Pt catalyst coatings).

6. Comparisons of the three models

In the single-zone model simulations, the combustion chamber is assumed to be a well-stirred reactor with uniform temperature, pressure and compositions. This model is applicable to the HCCI engine because here mixing is not a controlling factor. As shown in Table 6, the single-zone model analyses can predict the effects of catalytic combustion on the ignition timing of HCCI engine with good accuracy, and the computing time is shortest among the three models (all computations are on a Pentium 4, 2.8 GHz PC). However, because the in-cylinder temperature is actually non-uniform and the high temperature region in the center of the chamber is more responsible for the ignition, the single-zone model inevitably over-predicts the effects of catalytic combustion on the peak cylinder pressure and the NO_x emissions, and is not able to predict the effects of catalytic combustion on the emissions of HC and CO.

Because the multi-zone model accounts for the temperature inhomogeneity and thermal boundary layers, as well as the interactions between zones such as heat transfer and work, it has the ability to predict the effects of catalytic combustion on the emissions of HC, CO, and NO_x, and the computing time needed is not very long. But in this model, the detailed flow field is not considered, the chemical reactions are assumed to be unaffected by flow turbulence, and the initial mass and temperature distributions in zones have to be presumed including some uncertainties, so comparing with multidimensional model, the precision of the multi-zone model simulations is not very satisfactory.

In the multidimensional model simulations, the detailed flow field and the detailed chemical reactions are coupled, so it can predict the effects of catalytic combustion on the ignition timing, the emissions of HC, CO, and NO_x accurately, but it need the longest computing time among the three models.

7. Conclusions

In this paper, the combustion processes and emission characteristics of HCCI engines whose piston surfaces are coated with Pt catalyst are simulated systematically by modifying the SENKTN code of CHEMKTN chemical kinetics package, and adopting a detailed chemical kinetics mechanism that consists of surface reactions and gas reactions mechanisms. A single-zone model and a multi-zone model are built. The effects of catalytic combustion on the ignition timing, the combustion characteristics and the unburned HC, CO and NO_x emissions of a HCCI

engine are studied through these two models separately. Furthermore, by coupling the KTVA-3V package with the CHEMKIN and DETCHEM chemical kinetics packages, a multidimensional CFD model is built, and the effects of catalytic combustion on the ignition timing, the temperature field, the CO, HC concentration fields and the HC, CO and NO_x emissions of the HCCI engine are analyzed taking into account the inhomogeneity of temperature and species concentrations in the cylinder. The study produces following results:

(1) With the piston surface having Pt catalyst coatings, the ignition timing is advanced, and the peak temperature and the peak pressure in the cylinder are elevated slightly.
(2) With Pt catalyst coated on the piston surface, the HC and CO emissions are decreased but the NO_x emissions are increased.
(3) Compared with the case without catalyst coatings, the temperature and CO, HC concentration fields in the cylinder are more homogeneous when the piston surface has Pt catalyst coatings.

Acknowledgments

This research is supported by the National Key Basic Research Project of China (No. 2001CB209201).

References

[1] R.H. Stanglmaier, C.E. Robert. Homogeneous charge compression ignition (HCCI): benefits, compromises, and future engine applications, SAE Paper 1999-01-3682, 1999.
[2] B.F. Scott, N.A. Dennis, Development of a two-zone HCCI combustion model accounting for boundary layer effects, SAE Paper 2001-01-1028, 2001.
[3] B.F. Scott, N.A. Dennis, A four-stroke homogeneous charge compression ignition engine simulation for combustion and performance studies, SAE Paper 2000-01-0332, 2000.
[4] S.M. Aceves, D.L. Flowers, C.K. Westbrook, J.R. Smith, R.W. Dibble, M. Christensen, W.J. Pitz, B. Johansson, A multi-zone model for prediction of HCCI combustion and emission, SAE Paper 2000-01-0327, 2000.
[5] S.C. Kong, R.D. Reitz, M. Christensen, Modeling and experiments of HCCI engine combustion using detailed chemical kinetics with multidimensional CFD, SAE Paper 2001-01-1026, 2001.
[6] S. Seref, Examination of combustion characteristics and phasing strategies of a natural gas HCCI engine, Energy Convers. Manage. 46 (2005) 101–119.
[7] M. Christensen, P. Einewall, B. Johansson, Homogeneous charge compression ignition (HCCI) using isooctane, ethanol and natural gas—a comparison with spark-ignition operation, SAE Paper 972874, 1997.
[8] J. Gaffney, R. Sapienza, T. Butcher, C. Krishna, W. Marlow, T.O. Hare, Soot reduction in diesel engines: a chemical approach, Combust. Sci. Technol. 24 (1980) 89.
[9] R.H. Thring, Platium improves economy and reduces pollutants from a range of fuels, Catal. Engine 24 (1980) 126–133.
[10] Z. Hu, N. Ladommatos, In-cylinder catalysts—a novel approach to reduce hydrocarbon emissions from spark-ignition engines, SAE Paper 952419, 1995.
[11] Z. Hu. A mathematical model for in-cylinder catalytic oxidation of hydrocarbons in spark-ignition engines, SAE Paper 961196, 1996.
[12] A. Hultqvist, M. Christiensen, B. Johansson. The application of ceramic and catalytic coatings to reduce the unburned hydrocarbon emissions from a homogeneous charge compression ignition engine, SAE Paper 2000-01-1833, 2000.
[13] S.C. Kong, R.D. Reitz, Numerical study of premixed HCCI engine combustion and its sensitivity to computation mesh and model uncertainties, Combust. Theory Model. 7 (2003) 417–433.
[14] J. Bengtsson, P. Strandh, R. Johansson, P. Tunestal, B. Johansson, Closed-loop combustion control of homogeneous charge compression ignition (HCCI) engine dynamics, Int. J. Adaptive Control Signal Process. 18 (2004) 167–179.
[15] M. Sjoberg, J.E. Dec, An investigation into lowest acceptable combustion temperature for hydrocarbon fuels in HCCI engines, Proc. Comb. Inst. 30 (2005) 2719–2726.
[16] O. Deutschmann, http://detchem.com/mechanisms.
[17] R. Schwiedernoch, S. Tischer, O. Deutschmann, J. Warnatz, Experiment and numerical investigation of the ignition of methane combustion in a platinum-coated honeycomb monolith, Proc. Comb. Inst. 29 (2002) 1005–1011.
[18] M. Frenklach, T. Bowman, G. Smith, B. Gardiner, Gri-Mech 3.0, http://www.me.berkelev.edu/grimech/.
[19] L.E. William, A. Apoorva, A.L. George, Modeling of HCCI combustion and emissions using detailed chemistry, SAE Paper 2001-01-1029, 2001.
[20] R.J. Kee, F.M. Rupley, E. Meeks, J.A. Miller, CHEMKIN-III: A Fortran Chemical Kinetics Package for the Analysis of Gas-Phase Chemical and Plasma Kinetics, Sandia National Laboratories, Livermore, CA 94551-0969, 1996.
[21] O. Deutschmann, S. Tischer, S. Kleditzsch, C. Correa, D. Chatterjee, J. Wamatz, DETCHEM-Packagel.5.4. Steinbeis-Transferzentrum-Simulation Reaktiver Stromungen, Heidelberg, Germany, 2003.
[22] J.B. Heywood, Internal Combustion Engine Fundamentals, McGraw-Hill Book Company, 1988.
[23] G. Woschni, Universally applicable equation of the instantaneous heat transfer coefficient in the internal combustion engine, SAE Paper 670931, 1967.
[24] S.M. Aceves, D.L. Flowers, J. Martinez-Frias, J.R. Smith, C.K. Westbrook, W.J. Pitz, R.W. Dibble, J.F. Wright, W.C. Akinyemi, R.P. Hessel, A sequential fluid-mechanic chemical-kinetic model of propane HCCI Combustion, SAE Paper 2001-01-1027, 2001.
[25] S.M. Aceves, D.L. Flowers, E.L. Francisco, J. Martinez-Frias, J.E. Dec, M. Sjoberg, R.W. Dibble, R.P. Hessel, Spatial analysis of emissions sources for HCCI combustion at low loads using a multi-zone model, SAE Paper 2004-01-1910, 2004.
[26] S.C. Kong, R.D. Reitz, M. Christensen, Modeling the effects of geometry generated turbulence on HCCI engine combustion, SAE Paper 2003-01-1088, 2003.
[27] S.C. Kong, R.D. Reitz, Use of detailed chemical kinetics to study HCCI engine combustion with consideration of turbulent mixing effects, J. Eng. Gas Turbines Power 124 (2002) 702–707.
[28] S.C. Kong, M. Christensen, C.J. Runtland, Experiments and CFD modeling of direct injection gasoline HCCI engine combustion, SAE Paper 2002-01-1925, 2002.
[29] L. Alamos, KIVA-3V: a block-structured KTVA program for engines with vertical or canted values, LA-18818-MS, 1997.